Geocarto International

ISSN: (Print) (Online) Journal homepage: https://www.tandfonline.com/loi/tgei20

Spatial surface velocity pattern in the glaciers of Chandra Basin, western Himalaya

Lavkush Kumar Patel, Parmanand Sharma, Ajit T. Singh, Bhanu Pratap, Sunil Oulkar & Meloth Thamban

To cite this article: Lavkush Kumar Patel, Parmanand Sharma, Ajit T. Singh, Bhanu Pratap, Sunil Oulkar & Meloth Thamban (2021): Spatial surface velocity pattern in the glaciers of Chandra Basin, western Himalaya, Geocarto International, DOI: 10.1080/10106049.2021.1920627

To link to this article: https://doi.org/10.1080/10106049.2021.1920627

Accepted author version posted online: 23 Apr 2021.

Spatial surface velocity pattern in the glaciers of Chandra Basin, western Himalaya

Lavkush Kumar Patel[a], *, Parmanand Sharma[a], Ajit T. Singh[a,b], Bhanu Pratap[a], Sunil Oulkar[a,b], and Meloth Thamban[a]

[a]Ministry of Earth Sciences (MoES), Government of India, National Centre for Polar and Ocean Research, Headland Sada, Vasco-da-Gama, Goa, India

[b]School of Earth, Ocean and Atmosphere Sciences, Goa University, Taleigao Plateau, Goa, India

*Corresponding author Email: lavkushpatel@ ncpor.res.in

ABSTRACT

Himalayan glaciers are distinct by their surface characteristics such as debris-cover, supra/proglacial lakes, ice-cliff, and tributaries' contributions, thus complicating their surface velocity pattern and their response towards climate warming. While remote sensing and modelled surface velocity estimation are valuable on a larger scale, in-situ high-resolution data is crucial to validate them. In this study, four glaciers (Batal, Sutri Dhaka, Samudra Tapu, and Gepang Gath) from Chandra Basin were monitored to measure point-wise surface displacement using a static GNSS system during 2017-2018. Among them, the highest surface velocity was observed over Samudra Tapu (~64.3 ma^{-1}), a large and clean-type glacier, while the lowest was for Batal (~6.2 ma^{-1}), a small and debris-covered glacier. Our study highlighted the contrasting behaviour of lake-terminating and debris-covered glaciers for the surface velocity and also emphasize the additional control of the slope, supraglacial lake, debris thickness and convergence of glacier channels on the glacier surface velocity.

KEYWORDS glaciers; surface velocity; GNSS survey; Chandra basin; Himalaya

1. Introduction

Glacier velocity is the ice movement by deformation and sliding in response to gravitational forces and the ice-mass thickness (Cuffey & Paterson 2010). It varies from local to regional scale due to variable topography and climatic conditions (Watson & Quincey 2015). As glacier moves, it creates various surface and englacial features, including crevasses due to internal pressure gradients and stresses. Glacier ice moves from the top (bergschrund) to the lower terminus (snout) of a glacier, and this movement can be faster or slower, depending on the ice mass flux, slope, and surface melting (Cuffey & Paterson 2010). The shear stress and basal sliding can broadly explain the movement of a glacier. Additional factors are glacial topography, geometry, englacial channels, precipitation, debris cover, and supra/proglacial lakes that regulate the shear stress and basal sliding (Truffer 2004; Scherler et al. 2008; Cuffey & Paterson 2010; Haritashya et al. 2015). Further, the glacier velocity is also linked to surface morphology, which helps to distinguish between active and inactive ice on debris-covered glaciers, identify glacier surge events, and infer basal conditions using seasonal observations (Jiskoot et al. 2000).

Glacier surface velocity can be estimated via direct observations using a total station, Global Navigation Satellite System (GNSS) survey, time-lapse photography, unmanned aerial vehicle, and through satellite data (e.g., feature tracking, SAR interferometry) (Cuffey & Paterson 2010; Fahnestock et al. 2016). Several optical data processing tools (COSI-corr, ImGRAFT, SenDiT, SRFT, and CIAS) and Radar remote sensing techniques are being used for the glacier velocity

estimation (Rignot & Kanagaratnam 2006; Luckman et al. 2007; Scherler et al. 2008; Quincey & Glasser 2009; Bhambri et al. 2017; Singh et al. 2020). Some velocity data products like GoLIVE and ITS_LIVE are also available in the public domain (Dehecq et al. 2015; Fahnestock et al. 2016; Gardner et al. 2018). These velocity products have been estimated using satellite images with sub-pixel orthorectification and provided with reduced signal-to-noise ratio (Fahnestock et al. 2016). The available velocity data sets (GoLive, ITS_LIVE, etc.) are generally good and primarily used for the ice sheet, ice cap, and bigger valley glaciers. However, for the small valley glaciers like in Himalaya, the spatial resolution and topography are the main limiting factors, and even some of the valley glaciers are beyond the limits of feature tracking algorithms (King et al. 2018). In the Hindu Kush Himalaya (HKH) region, more than 70% of glaciers are smaller (< 0.5 km^2) in size (Bajracharya & Shrestha 2011), and employing the available velocity data products may lead to higher uncertainty to the end product. Due to the extreme challenges involved in field data collection in the high mountain region, the in-situ glaciers' surface velocity data is sparse, limiting our understanding of ice dynamics and changes in the mass balance of glaciers and associated processes (Ruiz et al. 2015). Therefore in-situ velocity data, especially for the small valley glaciers of the HKH region, are crucial to fill the above-said gap.

Most of the glacier velocity studies in the HKH region are based on satellite observations with larger spatial coverage (Kääb 2005; Dehecq et al. 2015; Fahnestock et al. 2016; Kraaijenbrink et al. 2016), and very few are supported by field observations (Wagnon et al. 2007; Azam et al. 2012; Pratap et al. 2012; Shukla et al. 2015). Several surface velocity reports using feature tracking and velocity-meter also exist for the glaciers of Chandra and Bhaga basin (Tiwari et al. 2014; Garg et al. 2017; Patel et al. 2019; Sahu & Gupta 2019a; Yellala et al. 2019; Singh et al. 2020). However, the primary focus of these studies was to analyse the annual and seasonal variability in surface velocities. Very few studies have highlighted the spatial variability in surface velocity at different altitudes using satellite-derived velocity data sets (Garg et al. 2017; Singh et al. 2020).

In this study, the surface velocity of the four major glaciers (Batal, Sutri Dhaka, Samudra Tapu, and Gepang Gath) of the Chandra basin, western Himalaya, have been estimated by using a precise GNSS survey between 2017 and 2018. The spatial variability in glacier surface velocity was assessed by analysing the surface characteristics (e.g., debris cover, proglacial lake, and convergence of glacial channels) of the glaceirs. Additionally, for regional comparison, the surface velocity data of selected glaciers were examined using the ITS_LIVE data sets. The extensive field data generated are unique and will be very usefull for the glaciological community to develop and validate vatious geospatial and model outputs.

2. Study Area

The Chandra basin is a major sub-basin of the upper Indus basin in the western Himalaya and spreads over 2440 km^2 with 201 glaciers in the basin (Sangewar & Shukla, 2009) covering ~700 km^2 of glacierised area (Figure 1). The basin represents a highly rugged terrain with lofty mountains and deeply dissected valleys. It lies in the monsoon-arid transition zone, which is considered as the northern limit of the Indian monsoon (Bookhagen & Burbank 2006). We selected four glaciers (Samudra Tapu, Sutri Dhaka, Gepang Gath, and Batal) covering nearly 116 km^2 of the glacierised area of the basin for the in-situ velocity measurements (Figure 1). These glaciers were selected based on their unique surface characteristics and topographical setting. Samudra Tapu and Sutri Dhaka are large and relatively debris-free glaciers (C-type glaciers), while the Batal is a small and highly debris-covered glacier (D-type glacier), and the Gepang Gath is a lake-terminating glacier. In this study, a glacier was categorised as 'debris-covered' if the ablation zone has a continuous cover of supraglacial debris across its entire width and/or the relative debris cover is >50% of the ablation zone (Kirkbride 2011).

The salient features of the selected glaciers in this study are given below:

Samudra Tapu: Samudra Tapu Glacier is 15.4 km long and covers an area of 78.9 ± 6.3 km^2. The altitude ranges from 4200 to 5900 m asl, with an average slope of 12° (Figure 1). It is a compound type glacier with two main channels, where the main channel flows from west to east and the other channel towards south to the northeast (Table 1 & Figure 1). The glacier is categorised as clean (C type), having a total ~8% debris-covered area (~22% of ablation area) mostly over the lower ablation zone. The satellite observations have shown a terminus fluctuation of ~ 33.2 ma^{-1} (1971-2014) and a mass balance of -1.1 ± 1.3 m w.e.a^{-1} (2000-2016) (Brun et al. 2017; Patel et al. 2017). The glacier is one of the fastest retreating glaciers in the Chandra basin. The recession of this glacier has generated a proglacial lake, which covers an area of 1.2 km^2 with a length and width of 1.9 km and 0.8 km, respectively.

Sutri Dhaka: Sutri Dhaka Glacier is 10.7 km long and covers 19.6 ± 1.6 km^2. The altitude varies from 4400-6200 m asl, with an average slope of 14.3° with the main valley facing northeast (Table 1 & Figure 1) (Sharma et al. 2016; Singh et al. 2017). It is a clean glacier (C-type) and has a significantly less (<5%) debris-covered area over the lower terminus (Figure 1). The terminus fluctuation (1971-2014) and mass balance (2000-2016) of this glacier are ~ 21.4 ma^{-1} and -1.11 ± 1.37 m w.e. a^{-1}, respectively (Brun et al. 2017; Patel et al. 2017).

Batal: Batal glacier is 6.5 km long and covers 4.4 ± 0.4 km^2 of glacier area with an altitudinal range of 4240-5800 m asl. The glacier's orientation is southwest to northeast, and the main valley faces northeast with an average slope of 17° (Table 1 & Figure 1). The glaciers have shown a terminus fluctuation (1971-2014) of ~13.3 ma^{-1} and a mass balance (2000-2016) of -0.62 ± 0.6 m w.e. a^{-1} (Brun et al. 2017; Patel et al. 2017; Sharma et al. 2016). Nearly 90% of the ablation zone is debris-covered with a debris thickness ranging up to 100 cm (Patel et al. 2016).

Gepang Gath: Gepang Gath glacier is 5.1 km long and covers an area of 11.05 ± 0.9 km^2. The altitude of the glacier ranges from 4000 to 5500 m asl with an average slope of 15° towards the northwest. The terminus fluctuation of the glacier is 23.3 ma^{-1} (1971-2014) and its mass balance 2000-2016 is -1.5 ± 1.2 m w.e. a^{-1} and has shown accelerated mass loss since 1971 (Brun et al. 2017; Patel et al. 2017). The Gepang Gath glacier is terminating in a large proglacial lake covering an area of 0.8 km^2 with a length and width of 2.2 km and 0.4 km, respectively. This lake has been expanding with a linear rate of ~35.4 m a^{-1}, and its volume has increased nearly 20 times since 1971 (Patel et al. 2017).

3. Data and Methodology

3.1. Glacier surface velocity using GNSS survey

In order to estimate the surface velocity of the glaciers, a network of bamboo stakes was installed over all four glaciers. The location and geo-coordinates of the stake markers were measured using a static GNSS survey using Leica (GS 10) dual-frequency DGPS (Figure 2). Details of stake locations and surface displacement are given in supplementary table S1.

The Leica GS 10 DGPS system works with 120 channels and can track 60 satellite signals, including excellent low altitude tracking capacity with very low noise. The system provides 3 mm ± 0.1 ppm (horizontal) to 3.5 mm ± 0.4 ppm (vertical) accuracy with static and post-processing methods. In this study, post-processing was adopted to get high-quality data with high accuracy. During the survey, one unit was fixed at the reference point of each glacier and used as a base (static) unit for continuous observation, while the second unit was used as a mobile unit (rover) and

measured the coordinates of each fixed point by taking reading for at least 15 minutes (900 seconds) at each point. Data from both systems were imported using Leica Geo office software for further processing. The processed data sets were used for the estimation of the glacier surface velocity. To estimate the displacement (d) of each fixed point between two observations (t_1 and t_2) for each point, we used the following equation:

$$d = \sqrt{(x_1 - x_2)^2 + (y_1 - y_2)^2} \qquad (1)$$

where the x_1 and x_2, y_1 and y_2 represent the coordinates of the fixed points of survey periods t_1 (2017) and t_2 (2018), respectively. The annual surface velocity for each fixed point was estimated by a simple displacement equation:

$$V_s = \frac{d \times 365}{(t_1 - t_2)} \qquad (2)$$

where V_s represents the annual surface velocity (m a^{-1}) for a particular fixed point. The velocity thus measured primarily represents the surface velocity for the year 2017 because of having the significant GNSS survey time during the ablation season for the year 2017.

3.2. Extraction of surface characteristics

Surface characteristics (debris cover, altitude, slope, aspect, and curvature) were extracted using ASTER GDEM V2 and Sentinel 2B datasets in selected glaciers. The Sentinel 2B (August 2018) satellite image was acquired from the USGS Earth Explorer portal (www.earthexplorer.usgs.gov/), and ASTER GDEM V2 from the Earth Remote Sensing Data Analysis Centre (ERSDAC), Japan. The spatial resolution of ASTER GDEM V2 is 30 meters, and the DEM has a vertical accuracy of 17 m (Tachikawa 2011). The Sentinel 2B data sets are available in a multispectral format with 13 bands in Visible, NIR, and SWIR spectrum with a spatial resolution of 10 to 60 m and a revisit time of 5 days (www.sentinel.esa.int). The debris cover was manually extracted using the visual tonal difference between the clean and debris-covered region (Bands: SWIR–NIR–Green/Red) in the processed images. The reflectance of rock in the SWIR band is higher than that of ice, making debris cover on glaciers appear in reddish or reddish-brown tone. By utilising these characteristics, debris-cover was identified through visual image interpretation (Patel et al. 2017).

3.3. Positional error in the stakes observations

The accuracy of DGPS data depends on the base and rover station set up and atmospheric conditions at the time of measurements (Quincey & Glasser 2009). In order to get better accuracy, the base station was fixed at an open location with a flat surface for more than 24 hours and rover measurements were taken during bright days with a clear line of sight. We tried to maintain a minimum of 15 satellites throughout our observations. The DGPS measurements showed a maximum error/uncertainty (Horizontal and Vertical) of 0.2 mm, a minimum of 90 mm, and a median of 0.4 mm for the year 2017 in point coordinate measurements. However, for the year 2018, it showed a maximum of 0.2 mm, a minimum of 40 mm, and a median of 0. 4 mm (Supplementary Figure S1). Positional errors in the stakes' horizontal position were measured using the following equation.

$$e = \sqrt{(x)^2 + (y)^2} \quad (3)$$

where x and y represent the positional accuracy in a particular point coordinate for 2017 and 2018, respectively. The analysis showed a mean positional error of 0.7 cm, with a maximum and minimum positional error of 9.1 and 0.03 cm.

3.4. Its_LIVE Data sets

The surface velocity data for selected glaciers and other sampled glaciers (used for only regional comparison) were extracted from the ITS_LIVE data sets (240 m spatial resolution) for the year 2017 available in public domain (Gardner et al. 2018). The selected glaciers are represented with their respective Randolph Glacier Inventory (RGI) ID in the supplementary figure S2. The ITS_LIVE products provide a globally comprehensive and temporally dense multi-sensor record of land and ice velocity with elevation information (Gardner et al. 2018). More details on the ITS_LIVE project and data sets are available in the NSIDC (https://its-live.jpl.nasa.gov/).

4. Results

4.4. Surface velocity patterns of glaciers in the Chandra basin

4.4.1. Samudra Tapu Glacier

The annual surface velocity of the Samudra Tapu Glacier ranged between 4.6 and 149.5 m a^{-1}, with a mean rate of ~64.3 m a^{-1} during 2017-2018 (Table 1). The glacier has two main tributaries - the one flowing south to northeast with a mean surface velocity of ~47.3 m a^{-1}, and the channel flowing west to east with a mean surface velocity of ~116.3 m a^{-1} (Figure 3). This glacier has experienced comparatively lower surface velocity over three altitudinal zones, i.e., over the lower terminus, at an altitude range of 4400-4600 m, and at 4700-4900 m asl (Figure 3). The surface velocity over the lower terminus area was significantly low (~4.5 m a^{-1}) during 2017-2018 (Figure 3). Within the altitudinal ranges 4400–4600 m asl, the average surface flow was ~55 m a^{-1} (ranging between 27.7 m a^{-1} and 85.7 m a^{-1}).

Compared to this, the observed average glacier surface velocity for the 4700-4900 m asl altitudinal range was 78.9 m a^{-1} (ranging between 52.9 and 135.8 m a^{-1}). Satellite images clearly showed that within this altitudinal range, the main channel has a higher flow (highly crevassed surface) than the secondary channel (Figure 4).

4.4.2. Sutri Dhaka Glacier

The annual surface velocity for the Sutri Dhaka Glacier ranged between ~15.4 and ~84.6 m a^{-1}, with an overall mean velocity of ~52.6 m a^{-1} (Table 1). This glacier showed a linear increase in surface velocity with elevation except for the altitudinal zone of 4700-4900 m asl (Figure 3). At this altitudinal zone, the mean surface velocity was ~40.3 m a^{-1}, which is comparatively lower than that of the subsequent elevation band of 5000-5200 m asl (~70.9 m a^{-1}). Higher surface velocity (~70.9 m a^{-1}) was observed near Equilibrium Line Altitude (5000 − 5200 m asl) and close to the accumulation zone.

4.4.3. Batal Glacier

Batal is a highly debris-covered glacier in the basin; therefore, the surface velocity was expected to be distinct from the clean glaciers. The annual glacier surface velocity estimated over the Batal glacier was 6.5 ma^{-1} with a minimum and maximum velocity of ~3.0 and ~10.6 ma^{-1}, respectively (Table 1 & Figure 3). There were no significant differences in surface velocities

between the lower part of the glacier (3.5 to 5 m a^{-1}) and the upper region (4.5 to 10.2 m a^{-1}) (Figure 3). Among all the four studied glaciers, the Batal glacier exhibited very low surface velocity.

4.4.4. Gepang Gath Glacier

The annual surface velocity of this lake-terminating glacier was ~26.5 ma^{-1}, with minimum and maximum surface velocities of ~11.3 and ~ 48.6 ma^{-1}, respectively (Table 1). In this glacier, the first 500 m zone (close to the proglacial lake) showed slightly higher surface velocity (~14.3 ma^{-1}) than the subsequent 500 m (~12.3 m a^{-1}). Thereafter, the surface velocity increased up to ~ 40 ma^{-1} (Figure 3).

5. Discussion

5.1. Inter and intra glacier comparison of surface velocities

Our study revealed significant differences in surface velocities among different glaciers as well as differences within a glacier itself. Among the studied glaciers, the maximum (~64.3 m a^{-1}) surface velocity was observed over the Samudra Tapu glacier, while minimum velocity (~6.2 m a^{-1}) was observed over the Batal glacier. Sutri Dhaka and Gepang Gath showed an average surface velocity of ~52.6 m a^{-1} and ~24.3 m a^{-1}, respectively (Table 1 and Figure 3). Samudra Tapu is the biggest glacier among the four, followed by Sutri Dhaka, Gepang Gath, and Batal. Both Samudra Tapu and Sutri Dhaka have larger accumulation areas, with tributaries contributing ice mass to the main trunk glacier. Therefore, our study suggests that larger glaciers in the Chandra basin are flowing faster than the smaller glaciers, potentially due to the large accumulation area feeding the glaciers and a high annual accumulation (Sam et al. 2018).

The convergence of tributary glaciers into larger glaciers also imposes a potential impact on the direction and velocity of glacial flow. We observed a sudden drop in the velocity at the confluence zones of the Samudra Tapu and Sutri Dhaka glaciers, which subsequently increased after the confluence in both the glaciers (Figure 3 and 4). The convergence contributes to the shear stress and strain over the main channel and caused deformation, seen in the form of crevasses over this altitudinal zone of the Samudra Tapu and Sutri Dhaka glaciers (Figure 4 a-d). The occurrence of ogives, crevasses, and moulins in this altitudinal zone have been verified during our field visits. The confluence zone blocks free movement and reduces the surface velocity, identified by the bulging surface.

Unlike the higher surface velocity in bigger and clean glaciers, the Batal Glacier had a low surface velocity (~6.2 m a^{-1}). The leading causes for such low velocity could be the extensive and thick debris cover over the entire ablation zone of the glacier, thin ice mass, and comparatively narrow valley. High debris cover (~95%) is one of the main factor impeding the surface velocity and the glacier's stagnant terminus (Rowan et al. 2015). High debris cover also reduces the ablation by insulating the glacier surface, so the meltwater to the base is not sufficient for basal lubrication. As a result, the basal sliding is effectively controlled by the reduced water input (Dunse et al. 2015). Further, the small glacier contains thin ice mass compared to bigger glaciers. Thus, the forces required to move the ice faster are relatively low due to low ice thickness and the resistance created by the base and the margin of a narrow glacial valley. In the case of the Gepang Gath, the higher glacier flow close to the proglacial lake indicates the impact of lake water over the glacial flow because of the reduction in buttressing.

The directly measured surface velocities of the studied glaciers in the Chandra basin are similar to the reported velocities of the big and small Himalayan glaciers in central and western Himalaya using remote sensing techniques (Gantayat et al. 2014; Satyabala 2016; Sam et al. 2018; Kumar et al. 2019). Using synthetic aperture data, Satyabala (2016) has reported the surface velocity of the Gangotri glacier in the range of 42.8 ± 4.2 m a^{-1} to 63.1 ± 5.4 m a^{-1} during 1991-2011. Similarly, using feature tracking and cross-correlation algorithm, Gantayat et al. (2014) reported a surface velocity range from 14-85 m a^{-1} (accumulation zone) to 20-30 m a^{-1} (ablation zone) for Gangotri Glacier. For the Siachen glacier in the Northwest Himalaya, Kumar et al. (2011) reported a high surface velocity of 156 m a^{-1} (43 cm/day) for the upper zone and 36.5 ma^{-1} (10 cm/day) for the lower zone. In the Chandra basin, similar surface velocities have been reported for the Chhota Shigri, the Bara Shigri, and the Samudra Tapu glaciers (Azam et al. 2012; Tiwari et al. 2014; Garg et al. 2017; Sahu and Gupta 2019a; Sahu and Gupta 2019b). However, Bara Shigri is a big glacier with a length of 27 km but has comparatively lower surface velocity (stagnant to 60 m a^{-1}), apparently due to extensive debris cover over the ablation zone (Sahu & Gupta 2019b).

5.2. Control of spatial surface characteristics on glacier surface velocity

5.2.1. Debris cover

Within the Chandra basin, nearly 29.5% of the glacierised area is debris covered, which is increasing annually due to enhanced glacier melting (Shukla et al. 2009; Patel et al. 2016). The debris cover also strongly influences the glacier ice ablation in the basin (Patel et al. 2017). The results showed a significant difference (90%) in surface velocity over the debris-covered region and debris-free region of the studied glacier (Figure 5). The surface velocity measured for the debris-covered region for studied glaciers was ~5.5 m a^{-1} with a range of ~3.07 to ~9.95 m a^{-1}, while for the debris-free region, the velocity ranges between ~12.9 and ~85.7 ma^{-1} with a mean velocity of ~ 51.7 ma^{-1} (Figure 5). Our data revealed ten times higher surface velocity over the debris-free area than the debris-covered area. In order to minimise the altitudinal bias in the comparative analysis, the analysis was carried out with the survey points (n = 28) below 4700 m asl for debris-covered and clean glaciers. The elevation below 4700 m asl is the region where clean and debris-cover occupies similar percentage of a 'glaciers' area. This analysis clearly showed that the surface velocity over the clean ice (~33.2 m a^{-1}) was much higher (nearly six times) than the debris-covered area (~5.5 ma^{-1}).

To strengthen the in situ observations and compare the surface velocity pattern over larger numbers of glaciers in the region, glacier-wide surface velocities were extracted from 12 glaciers using the ITS_LIVE data in the western Himalaya including four in situ studied glaciers (Supplementary Figure S2). The average annual ITS_LIVE velocities for the studied four glaciers were comparatively lower than the DGPS observations (Figure 6). The reasons for apparent underestimation by the ITS_LIVE data compared to in situ DGPS data for these glaciers may be due to its coarser spatial resolution (240 m). It has also been observed that the ITS_LIVE data sets have higher differences for smaller glaciers and has minor difference for Samudra Tapu, the largest glacier. The expected cause for this difference may be the satellite image resolution used for the generation of the velocity data sets and the topography effects of the small glaciers.

Among twelve glaciers analysed using the ITS_LIVE data, the debris-covered glaciers showed comparatively low surface velocity (<16 m a^{-1}) than the clean glaciers (>20 m a^{-1}) (Figure 7 a & b). As discussed previously, the lower surface velocity over the debris-covered glaciers is attributed to the thick debris, thin ice mass, and confined narrow valleys. Typically thin ice mass in debris-covered glaciers cannot exert optimum pressure to move faster due to increased basal and marginal resistance. Additionally, coupling of thin ice mass with thick debris in the narrow valley exerts higher marginal resistance which impede the surface velocity (Cuffey & Paterson 2010). Further, thes debris-covered glaciers' low-velocity zones are attributed to evolving supraglacial

ponds and open ice cliffs (Banerjee & Shankar 2013). Similar conditions were observed in Samudra Tapu and Batal glaciers (Figure 4 e, and f), where many supraglacial ponds and open ice cliffs were found over the debris-covered area. Such developments of supraglacial ponds and ice cliffs have also been reported in debris cover zone associated with lower surface velocity for the Zanskar basin, western Himalaya (Scherler et al. 2011; Banerjee & Shankar 2013; Bhushan et al. 2018), and central and eastern Himalaya (Kääb 2005; Kraaijenbrink et al. 2016). Kraaijenbrink et al. (2016) have observed a maximum surface velocity of 6 and 2.5 ma^{-1} (winter and summer maximum respectively) over debris-covered Lirung Glacier in Nepal, whereas Kääb (2005) has reported <20 m a^{-1} surface velocity for the debris-covered glaciers in Bhutan. The present study reveals that the debris cover influences the surface flow of the glacier and consequently could alter the response of glaciers to the warming climate.

5.2.2. Presence of Proglacial Lake

Among the four in-situ studied glaciers, two glaciers, i.e., Samudra Tapu and Gepang Gath, have large proglacial lakes (Figure 1 a&d). Although both the glaciers are lake terminating, the mean surface velocity for the Samudra Tapu glacier is much higher (~64.3 m a^{-1}) than the Gepang Gath Glacier (~26.5 ma^{-1}). However, close to the terminus (up to 1.5 km from snout), the surface velocity of the Gepang Gath was much higher (~20 m a^{-1}) than Samudra Tapu (~5 m a^{-1}) although the lower region of both the glaciers are debris-covered (Figure 1 a&d, Figure 4 f & g). Such differences in surface velocity near the terminus are due to the substantial impact of the Gepang Gath glacier's proglacial lake than that of Samudra Tapu glacier. The calving processes are more dominant in Gepng Gath than Samudra Tapu (Patel et al. 2017) due to the deeper (45 m) water column and the larger area and higher coverage of ice–water interface at the lower terminus in Gepang Gath glacier. Studies have shown a strong positive correlation between calving processes and surface velocity (Carrivick & Tweed 2013, King et al. 2018); therefore, increased calving events could have accelerated the surface velocity near to terminus over the Gepang Gath glacier. The terminal part of this glacier is highly deformed due to higher surface velocity, observed in the form of several baby crevasses close to the terminus (Figure 4g). Compared to this, over Samudra Tapu, there are many ice cliffs and supraglacial ponds in the lower region, which indicate low surface velocity over this region. The proglacial lake of Samudra Tapu has limited impact on the terminus due to the shallow (~ 3 m) water at the ice-water interface with a small cross-section area/coverage area. Energy transfer to the glacier ice during ice-water interaction accelerates calving processes and, consequently, high surface velocity (Owen and England 1998; Patel et al. 2017). Recent studies have demonstrated that the proglacial lake of Gepang Gath glacier has expanded nearly 20 times in area and volume during 1971 − 2014 due to the combined impact of calving and high glacier surface velocity (Patel et al. 2017).

The ITS_LIVE surface velocity (data sets for the glaciers with proglacial lakes in the western Himalaya (8 glaciers; Supplementary Figure S2) showed significant differences in surface velocities. The average surface velocity for the selected glaciers ranged from 0.9 − 60.6 m a^{-1} (Figure 8 a, &b). Among these glaciers, some have very slow surface velocity in the lower zone while others have comparatively higher velocity in the lower zone (Figure 8b). These observations underscore the strong influence of lake calving over the glacier velocity and are consistent with King et al. (2018), who observed the high velocity over the glaciers having proglacial lakes and low velocity over the glaciers with supraglacial lakes. Studies conducted over nearly 200 glaciers in Greenland have reported similar results, showing significantly high surface velocity over the calving glaciers compared to land-terminating glaciers (Moon et al. 2012).

5.2.3. Altitude variation

Maximum (~63.01 m a^{-1}) surface velocity was observed at the altitude >5000 m, and the minimum (~12.79 ma^{-1}) was at < 4500 m asl altitude (Figure 9a). The observed high velocity above 5000 m altitude was within the theoretically expected higher velocity near the snowline (Cuffey & Paterson 2010). The high-velocity regions in studied glaciers are characterised by surface features such as crevasses (Figure 4 a- d). The higher altitudes experienced more mass load over glaciers due to high accumulation and avalanche contributions (Sam et al. 2018), consequently increasing the stress that causes higher glacial flow. The high velocity in the region indicates increased basal sliding and subglacial deformation due to reduced friction, which occurs when meltwaters penetrate the glacier bed. Several studies have also observed the dominant elevation control on glacial flow over the Baspa basin and Siachin glaciers (Kumar et al. 2011; Sam et al. 2018).

5.2.4. Surface slope and aspect

The uneven topography of this basin leads to a significant variation in slope over the glacier surface (Figure 9b). The maximum velocity was observed over the slope class 5-10° (50.9 ma^{-1}), followed by the 0-5° (45.2 ma^{-1}) class. Since the data points are significantly less in slope class >15° (n = 2; Supplementary Table S 2), it is difficult to explain the behaviour of glacier velocity in this slope class. However, the ITS_LIVE data showed contrast behaviour with lower velocity in this class (30.7 ma^{-1}). It is expected that the steeper parts of the glacier surface have higher surface velocity, but observation revealed lesser velocity over the slope classes 10-15°, and >15°. However, the present study do not confirm this attribute since statistically fewer surveyed points comes from higher slope classes (n = 2), which also belongs lower altitude zones (mean altitude = 4660 m asl) (Supplementary Table 2), that is expected to have low ice thicknesses. Studies have shown that the higher velocity over the steep slope is due to the increased shear stress and thick ice mass (Marshall et al. 2011). As a result, thin ice masses may be one of the possible reasons for lower surface velocity in the higher slope classes (Figure 9b and Supplementary Table 2).

The present study showed that the glaciers flowing towards the west and south had experienced the highest surface velocity (~72.1 m a^{-1}). Compared to these, east-flowing glaciers experienced the lowest surface velocity (~44.2 ma^{-1}) (Figure 9c). South facing glaciers receive maximum solar radiation over a year and experience higher melting. The west-facing glaciers receive large accumulation due to the windward side and less solar radiation due to the shading effect (Hambrey & Glasser 2012; Sam et al. 2018; Yellala et al. 2019). This is in agreement with our results of higher surface velocity over the west and south-facing glaciers.

6. Conclusions

In situ measurements of the surface velocity of glaciers are essential to understand their response to changing climate, but are sparse in the Himalayan region due to factors like remoteness, inaccessibility caused by high altitudes, harsh climatic conditions and undulated terrain. Four glaciers from the Chandra basin (western Himalaya) with distinct topographic characteristics were studied for spatial variability in surface velocity. In situ surface velocity was measured using static GNSS surveys and compared with the spatial velocity pattern obtained from remote sensing techniques. Present study revealed that velocities over the large and clean glaciers were relatively higher compared to the smaller and debris-covered glaciers. The large glaciers have a high ice thickness, larger accumulation area, and therefore receive a higher amount of precipitation, which potentially increase the basal sliding and subglacial deformation due to increased shear stress. Our study showed that the debris-covered region of the glaciers have low velocity and are close to the stagnant phase. The debris cover significantly influences the glacial flow when associated with thin ice mass, narrow valley, and reduced surface melt. Similarly, the proglacial lakes potentially control the surface velocity in the lower ablation zone, especially close to the lower terminus, due to the

calving processes. Glacier surface velocity showed a gradual increment along with increasing altitude and distance from the snout. Our study reveals that the most significant factors influencing the glacier surface velocity in the Chandra basin are altitude, accumulation area, debris cover, and proglacial lakes.

References

Azam MF, Wagnon P, Ramanathan A, Vincent C, Sharma P, Arnaud Y, Linda A, Pottakkal JG, Chevallier P, Singh VB, Berthier E. 2012. From balance to imbalance: A shift in the dynamic behaviour of Chhota Shigri glacier, western Himalaya, India. J Glaciol. 58 (208):315-324.

Bajracharya SR, Shrestha B (eds). 2011. The status of glaciers in the Hindu Kush-Himalayan region. Kathmandu: ICIMOD, ISBN 978 92 9115 215 5.

Banerjee A, Shankar R. 2013. On the response of Himalayan glaciers to climate change. J Glaciol. 59(215): 480-490.

Bhambri R, Hewitt K, Kawishwar P, Pratap B. 2017. Surge-type and surge-modified glaciers in the Karakoram. Sci. Rep. 7 (1):1-14.

Bhushan S, Syed TH, Arendt AA, Kulkarni AV, Sinha D. 2018. Assessing controls on mass budget and surface velocity variations of glaciers in western Himalaya. Sci. Rep. 8 (1):8885.

Bookhagen B, Burbank DW. 2006. Topography, relief, and TRMM-derived rainfall variations along the Himalaya. Geophys. Res. Lett. 33 (8): L08405.

Brun F, Berthier E, Wagnon P, Kääb A, Treichler D. 2017. A spatially resolved estimate of high mountain Asia glacier mass balances from 2000 to 2016. Nat. Geosci. 10(9):668-673.

Carrivick JL, Tweed FS. 2013. Proglacial lakes: Character, behaviour and geological importance. Quat. Sci. Rev. 78:34-52.

Cuffey KM, Paterson WSB. 2010. The physics of glaciers, 4 ed.: Academic Press.

Dehecq A, Gourmelen N, Trouve E. 2015. Deriving large-scale glacier velocities from a complete satellite archive: Application to the Pamir–Karakoram–Himalaya. Remote Sens. Environ. 162:55-66.

Dunse T, Schellenberger T, Hagen JO, Kääb A, Schuler TV, Reijmer CH. 2015. Glacier-surge mechanisms promoted by a hydro-thermodynamic feedback to summer melt, Cryosphere, 9:197–215.

Fahnestock M, Scambos T, Moon T, Gardner A, Haran T, Klinger M. 2016. Rapid large-area mapping of ice flow using Landsat 8. Remote Sens. Environ. 185, 84-94.

Gantayat P, Kulkarni AV, Srinivasan J. 2014. Estimation of ice thickness using surface velocities and slope: A case study at Gangotri glacier, India. J Glaciol. 60 (220):277-282.

Gardner AS, Moholdt G, Scambos T, Fahnstock M, Ligtenberg S, Van Den Broeke M, Nilsson J. 2018. Increased west antarctic and unchanged east antarctic ice discharge over the last 7 years. Cryosphere, 12 (2):521-547.

Garg PK, Shukla A, Tiwari RK, Jasrotia AS. 2017. Assessing the status of glaciers in part of the Chandra basin, Himachal Himalaya: A multiparametric approach. Geomorphology 284, 99-114.

Hambrey MJ, Glasser NF. 2012. Discriminating glacier thermal and dynamic regimes in the sedimentary record. Sediment. Geol. 251-252:1-33.

Haritashya UK, Pleasants MS, Copland L. 2015. Assessment of the evolution in velocity of two debris-covered valley glaciers in Nepal and New Zealand. Geogr. Ann. Ser. A Phys. Geogr. 97(4):737-751.

Jiskoot H, Murray T, Boyle P. 2000. Controls on the distribution of surge-type glaciers in Svalbard. J Glaciol. 46(154):412-422.

Kääb A. 2005. Combination of SRTM3 and repeat ASTER data for deriving alpine glacier flow velocities in the Bhutan Himalaya. Remote Sens. Environ. 94(4):463-474.

King O, Dehecq A, Quincey D, Carrivick J. 2018. Contrasting geometric and dynamic evolution of lake and land-terminating glaciers in the central Himalaya. Global Planet. Change. 167:46-60.
Kirkbride MP. 2011. Debris-covered glaciers. In V. P. Singh, P. Singh, & U. K. Haritashya (Eds.), Encyclopedia of snow, ice and glaciers. Springer. 190-192.
Kraaijenbrink P, Meijer SW, Shea JM, Pellicciotti F, De Jong SM, Immerzeel WW. 2016. Seasonal surface velocities of a Himalayan glacier derived by automated correlation of unmanned aerial vehicle imagery. Ann. Glaciol. 57 (71):103-113.
Kumar P, Saharwardi MS, Banerjee A, Azam MF, Dubey AK, Murtugudde R. 2019. Snowfall variability dictates glacier mass balance variability in Himalaya-Karakoram. Sci. Rep. 9(1):18192.
Kumar, V., Venkataramana, G. & Høgda, K.A., 2011. Glacier surface velocity estimation using SAR interferometry technique applying ascending and descending passes in Himalayas. Int. J. Appl. Earth Obs. Geoinf. 13 (4), 545-551.
Luckman A, Quincey D, Bevan S. 2007. The potential of satellite radar interferometry and feature tracking for monitoring flow rates of Himalayan glaciers. Remote Sens. Environ.111(2):172-181.
Marshall SJ, White EC, Demuth MN, Bolch T, Wheate R, Menounos B, Beedle MJ, Shea JM. 2011. Glacier water resources on the eastern slopes of the Canadian rocky mountains. Can. Water Resour. J. 36(2):109-134.
Moon T, Joughin I, Smith B, Howat I. 2012. 21st-century evolution of Greenland outlet glacier velocities. Science. 336 (6081):576.
Owen LA, England J. 1998. Observations on rock glaciers in the Himalayas and Karakoram mountains of northern Pakistan and India. Geomorphology, 26(1):199-213.
Patel A, Dharpure JK, Snehmani, Ganju A. 2019. Estimating surface ice velocity on Chhota Shigri glacier from satellite data using Particle Image Velocimetry (PIV) technique. Geocarto Int. 34(4):335-347.
Patel LK, Sharma P, Laluraj CM, Thamban M, Singh A, Ravindra R. 2017. A geospatial analysis of Samudra tapu and Gepang Gath glacial lakes in the Chandra basin, western Himalaya. Nat. Hazard. 86(3):1275-1290.
Patel LK, Sharma P, Thamban M, Singh A, Ravindra R. 2016. Debris control on glacier thinning—a case study of the Batal glacier, Chandra basin, western Himalaya. Arabian J. Geosci. 9(4):309.
Pratap B, Sharma P, Patel L, Singh AT, Gaddam VK, Oulkar S, Thamban M. 2019. Reconciling High Glacier Surface Melting in Summer with Air Temperature in the Semi-Arid Zone of western Himalaya. Water, 11:1561.
Pratap B, Srivastava D, Dobhal D, Swaroop S. 2012. Flow characteristics of the Dunagiri glacier, Garhwal Himalaya. Jour. Ind. Geol. Cong. 4(1):113-118.
Quincey DJ, Glasser NF. 2009. Morphological and ice-dynamical changes on the Tasman glacier, New Zealand, 1990–2007. Global Planet. Change. 68(3):185-197.
Rignot E, Kanagaratnam P. 2006. Changes in the velocity structure of the Greenland ice sheet. Science. 311(5763):986.
Rowan AV, David L, Duncan E, Quincey J, Glasser NF. 2015. Modelling the feedbacks between mass balance, ice flow and debris transport to predict the response to climate change of debris-covered glaciers in the Himalaya. Earth Planet. Sci. Lett. 430:427-438.
Ruiz L, Berthier E, Masiokas M, Pitte P, Villalba R. 2015. First surface velocity maps for glaciers of monte tornado, north Patagonian Andes, derived from sequential pléiades satellite images. J Glaciol. 61(229):908-922.
Sahu, R. & Gupta, R., 2019a. Surface velocity dynamics of Samudra Tapu glacier, India from 2013 to 2017 using Landsat-8 data. ISPRS Annals of the Photogrammetry, Remote Sensing, Spatial Information Sciences, 4:75-81.

Sahu R, Gupta RD. 2019b. Spatiotemporal variation in surface velocity in Chandra basin glacier between 1999 and 2017 using Landsat-7 and Landsat-8 imagery. Geocarto Int. 1:21.
Sam L, Bhardwaj A, Kumar R, Buchroithner MF, Martín-Torres FJ. 2018. Heterogeneity in topographic control on velocities of western Himalayan glaciers. Sci. Rep. 8(1): 12843.
Sangewar CV, Shukla SP. 2009. Inventory of the Himalayan Glaciers: A Contribution to the International hydrological programme. Special publication No.34, Geological Survey of India pp 155-179.
Satyabala SP. 2016. Spatiotemporal variations in surface velocity of the Gangotri glacier, Garhwal Himalaya, India: Study using synthetic aperture radar data. Remote Sens. Environ. 181:151-161.
Scherler D, Bookhagen B, Strecker MR. 2011. Spatially variable response of Himalayan glaciers to climate change affected by debris cover. Nat. Geosci. 4(3):156-159.
Scherler D, Leprince S, Strecker MR. 2008. Glacier-surface velocities in alpine terrain from optical satellite imagery—accuracy improvement and quality assessment. Remote Sens. Environ. 112 (10):3806-3819.
Sharma P, Patel LK, Ravindra R, Singh A, Mahalinganathan K, Thamban M. 2016. Role of debris cover to control specific ablation of adjoining Batal and Sutri Dhaka glaciers in Chandra basin (Himachal Pradesh) during peak ablation season. J. Earth Syst. Sci. 125 (3), 459-473.
Shukla A, Gupta RP, Arora MK. 2009. Estimation of debris cover and its temporal variation using optical satellite sensor data: A case study in Chenab basin, Himalaya. J Glaciol. 55 (191):444-452.
Shukla S, Mishra R, Chitranshi A. 2015. Dynamics of Hamtah glacier, Lahaul & Spiti district, Himachal Pradesh. Journal of Indian Geophysical Union, 19 (4):414-421.
Singh AT, Laluraj C, Sharma P, Patel LK, Thamban M. 2017. Export fluxes of geochemical solutes in the meltwater stream of Sutri Dhaka glacier, Chandra basin, western Himalaya. Environ. Monit. Assess.189 (11):555.
Singh G, Nela BR, Bandyopadhyay D, Mohanty S, Kulkarni AV. 2020. Discovering anomalous dynamics and disintegrating behaviour in glaciers of Chandra-Bhaga sub-basins, part of western Himalaya using DinSAR. Remote Sens. Environ. 246:111885.
Tachikawa T, Hato M, Kaku M, Iwasaki A. 2011. The characteristics of ASTER GDEM version 2, Proc. IGARSS 2011 Symposium, Vancouver, Canada, 24–29 July 2011, 3657–3660.
Tiwari, R., Gupta, R. & Arora, M., 2014. Estimation of surface ice velocity of Chhota Shigri glacier using sub-pixel ASTER image correlation. Curr Sci. 106 (6):853-859.
Truffer M. 2004. The basal speed of valley glaciers: An inverse approach. J Glaciol. 50 (169):236-242.
Wagnon P, Linda A, Arnaud Y, Kumar R, Sharma P, Vincent C, Pottakkal JG, Berthier E, Ramanathan A, Hasnain SI. 2007. Four years of mass balance on Chhota Shigri glacier, Himachal Pradesh, India, a new benchmark glacier in the western Himalaya. J Glaciol. 53 (183):603-611.
Watson CS, Quincey DJ. 2015. Glacier movement: British Society for Geomorphology.

Yellala A, Kumar V, Høgda KA. 2019. Bara Shigri and Chhota Shigri glacier velocity estimation in western Himalaya using Sentinel-1 SAR data. Int. J. Remote Sens., 40 (15):5861-5874.

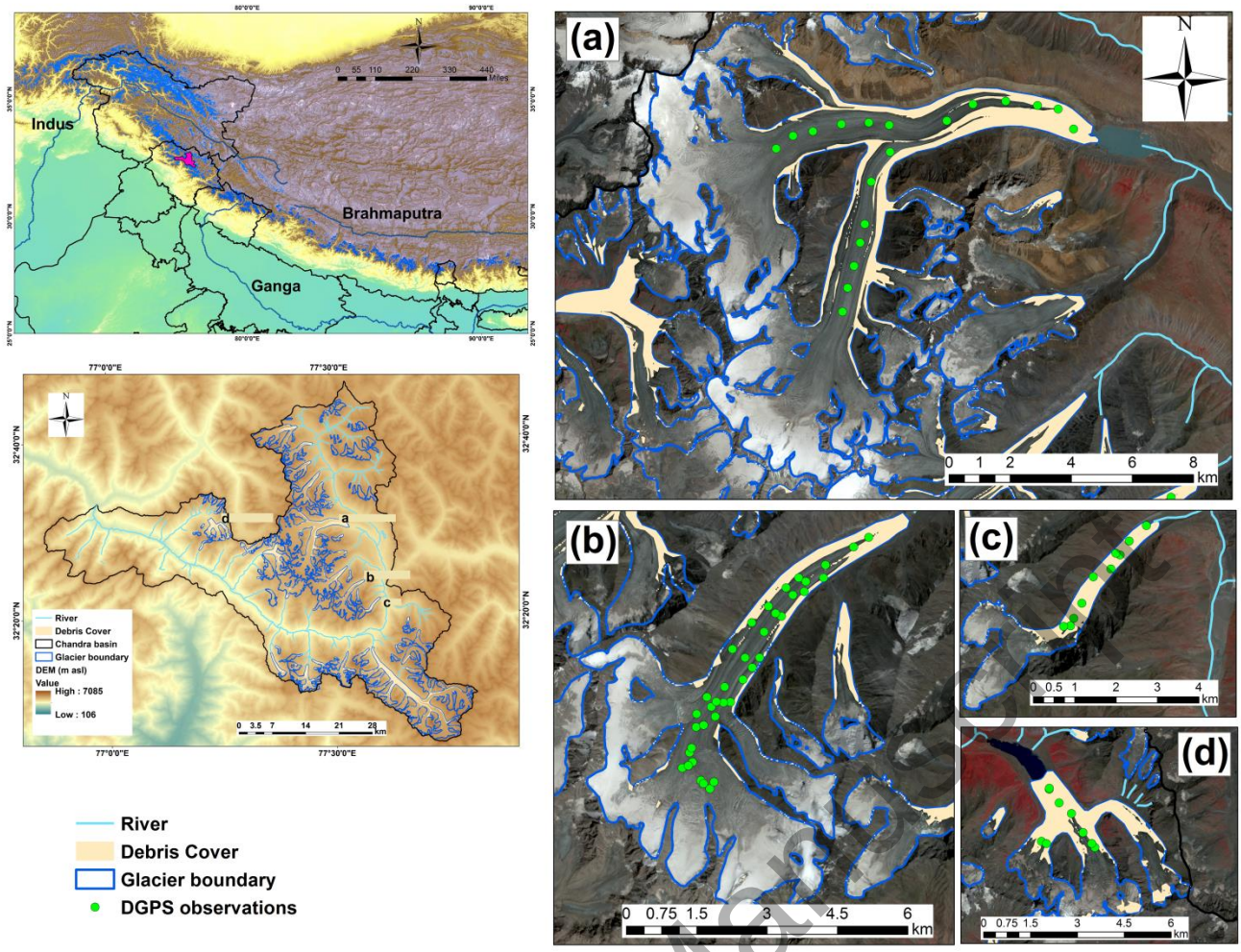

Figure 1. The location of the Chandra basin in the HKH region, and hypsometry and glaciers' outline with the location of the selected glaciers for the study from the Chandra basin. The right panels show the spatial distribution of the fixed bamboo stakes over the (a) Samudra Tapu, (b) Sutri Dhaka, (c) Batal, and (d) Gepang Gath glaciers (Background data: SRTM (for HKH), GDEM V2 (Chandra basin), and Sentinel 2B data for the glaciers for the year 2018 with10m spatial resolution. The debris cover over the glaciers is highlighted in light yellow shading.

Figure 2. The location of the Chandra basin in the HKH region, hypsometry and glaciers' outline with the location of the selected glaciers from the Chandra basin. The right panels show the spatial distribution of the fixed bamboo stakes over the (a) Samudra Tapu, (b) Sutri Dhaka, (c) Batal, and (d) Gepang Gath glaciers (Background data: SRTM (for HKH), GDEM V2 (Chandra basin), and Sentinel 2B data for the glaciers for the year 2018 with 10 m spatial resolution. The debris cover over the glaciers is highlighted in light yellow shading.

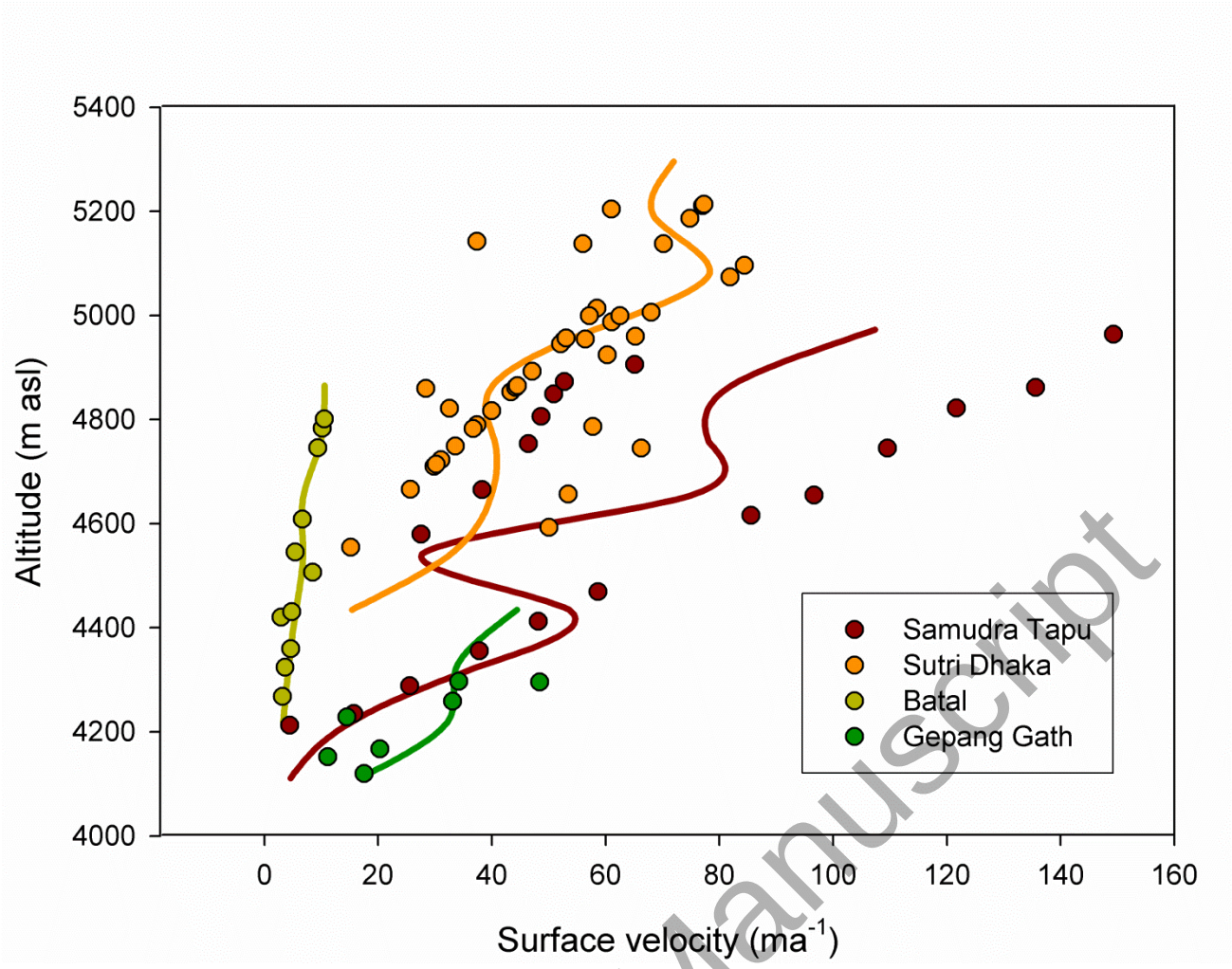

Figure 3. The DGPS observations over the ablation (a) and accumulation (b) zones of the Sutri Dhaka glacier. (c) The region below 5200 m asl (ablation zone) of the Sutri Dhaka glacier.

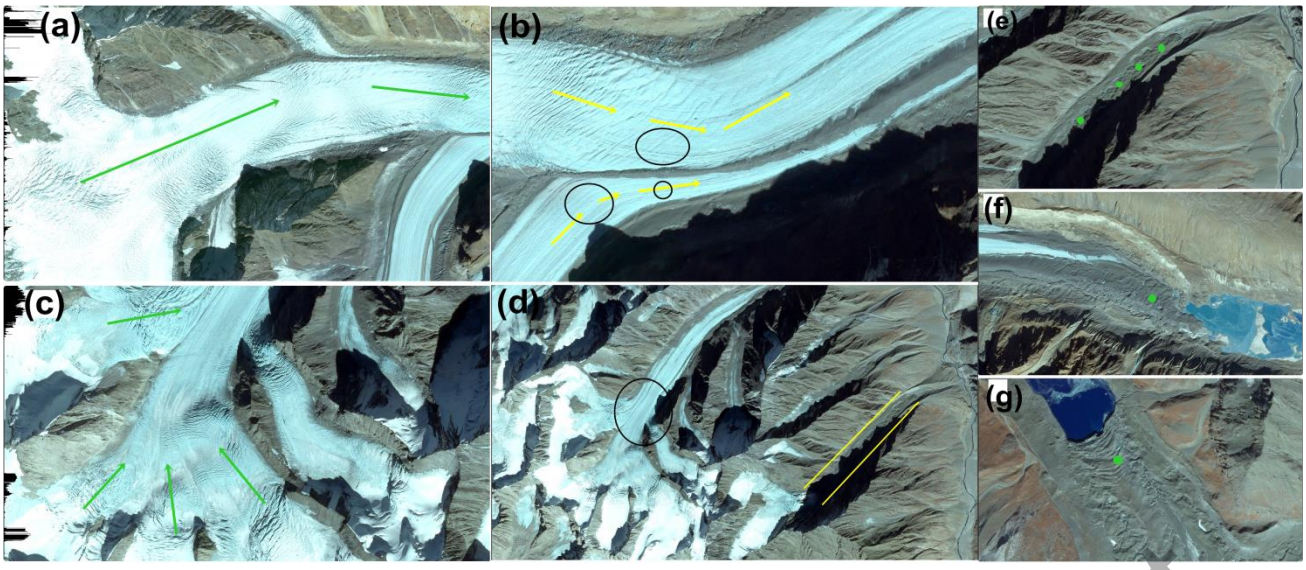

Figure 4. The surface velocity of the studied glaciers versus altitude. The colored circles represent the DGPS observation points while the colored lines provide the average surface velocity for particular glaciers (similar color has been given for the circle and line for individual glaciers). Detailed data is provided in supplementary table S1.

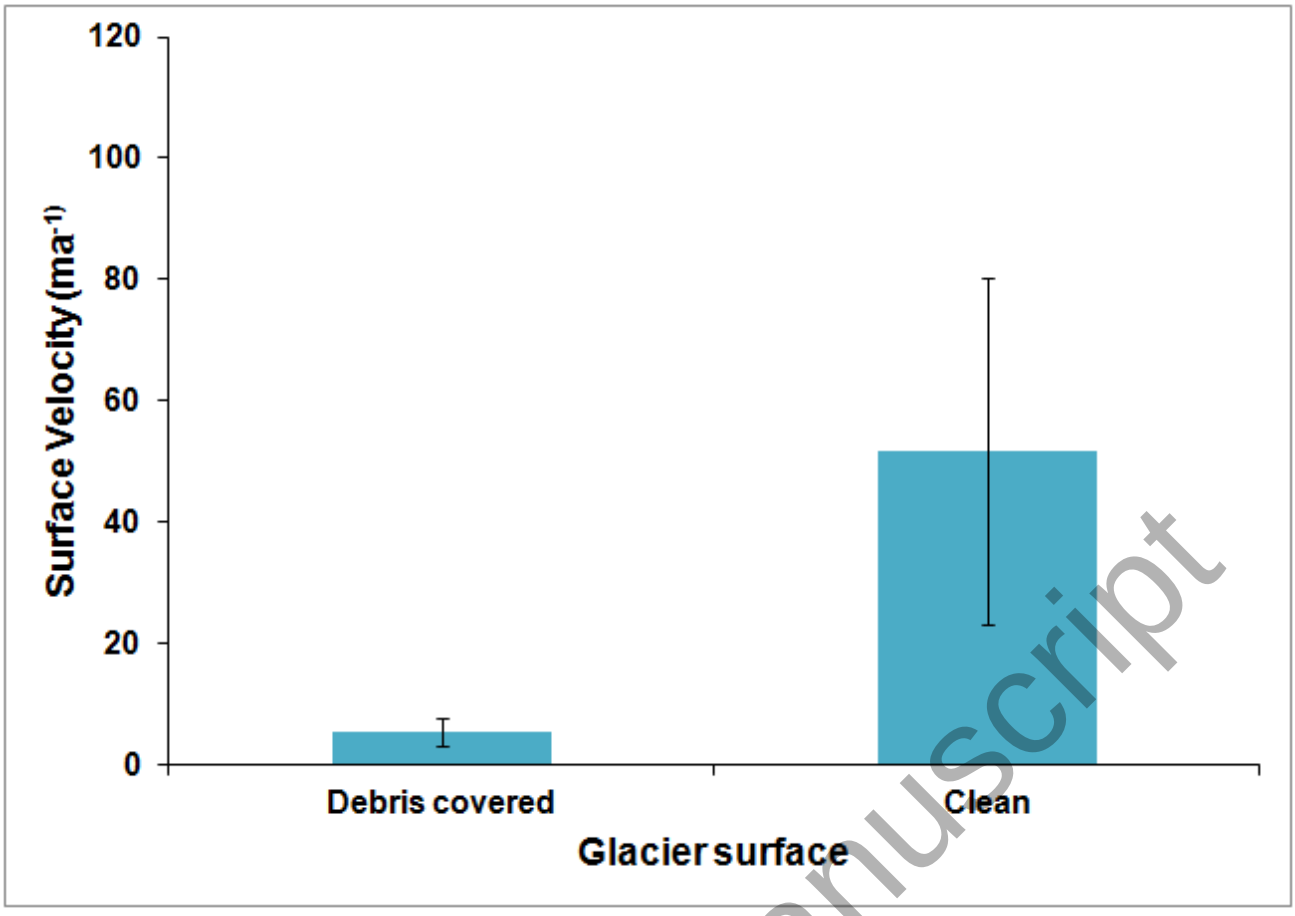

Figure 5. Average glacier surface velocity of the debris-covered and clean region of the measured fixed points over the selected glaciers. Here the average represents the surface velocity of a particular point from the glacier surface type (clean or debris cover) not the individual glacier.

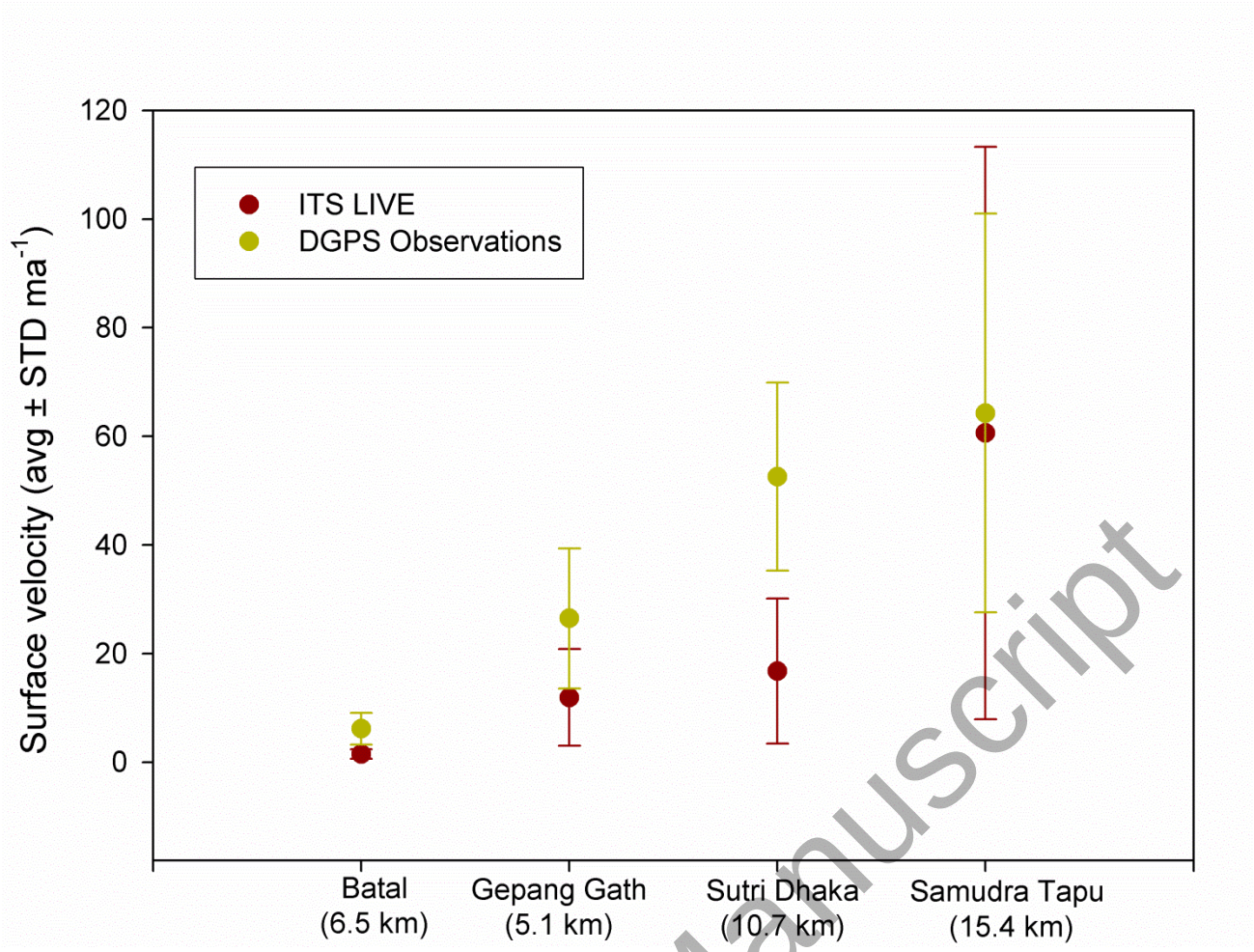

Figure 6. Comparison of ITS_LIVE data and DGPS measurements on the average annual surface velocity of the four glaciers of the Chandra basin for 2017.

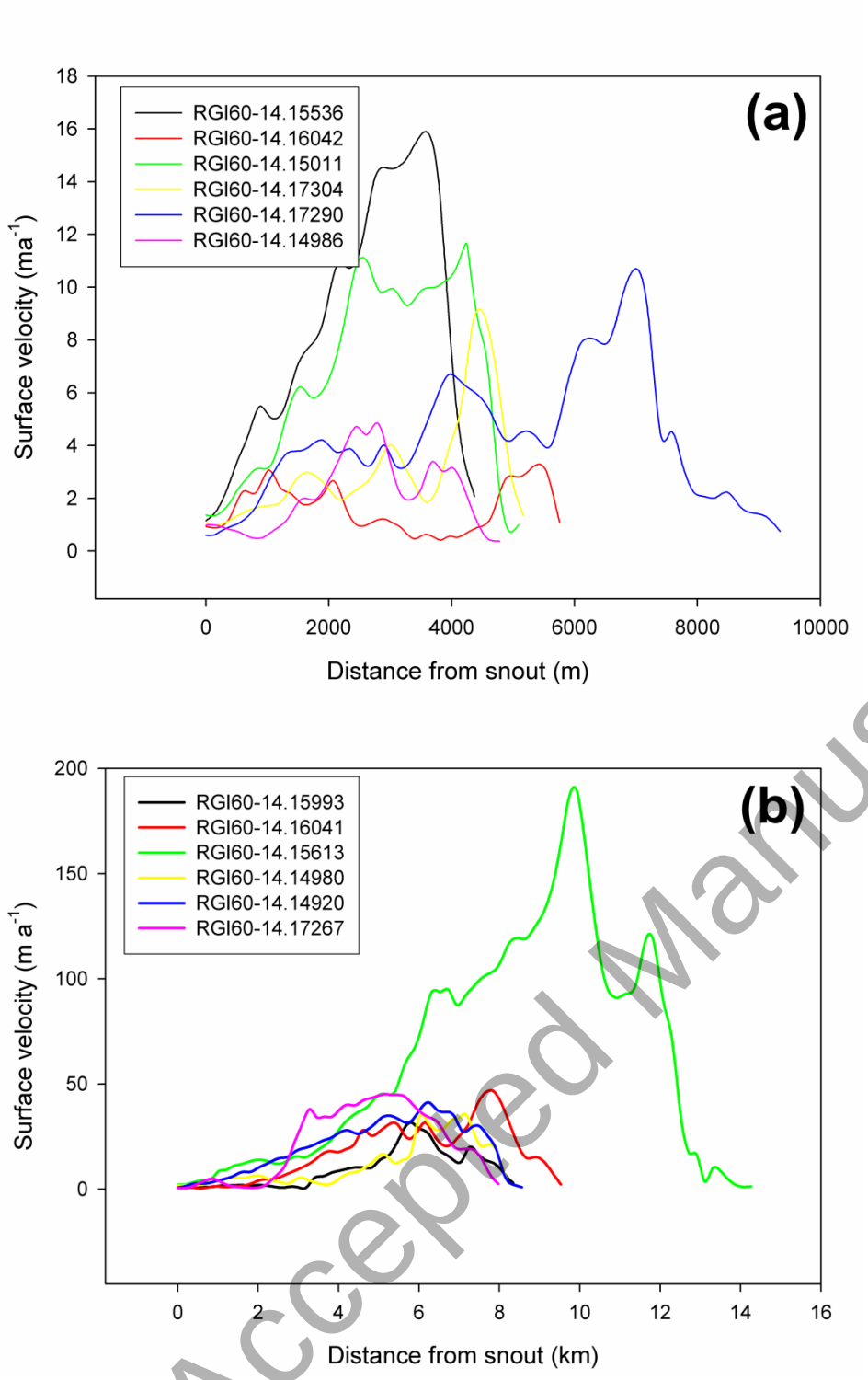

Figure 7. Variation in the glacier surface velocity of (a) debris-covered and (b) clean glaciers of Western Himalaya acquired from ITS_LIVE data sets. (The glaciers are represented with Randolph glacier Inventory (RGI) ID and the location of the selected glaciers has been provided in supplementary figure S2).

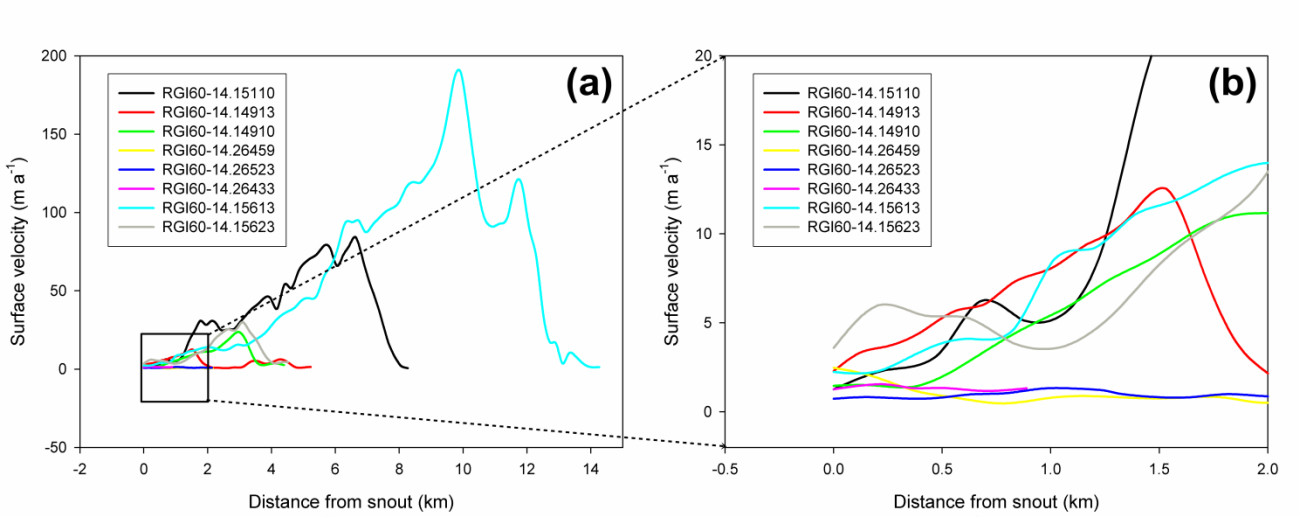

Figure 8. The surface velocity of the selected lake-terminating glaciers of the Western Himalaya using ITS_LIVE data (The glaciers are represented with Randolph glacier Inventory (RGI) ID and the location of the selected glaciers has been provided in Figure S2).

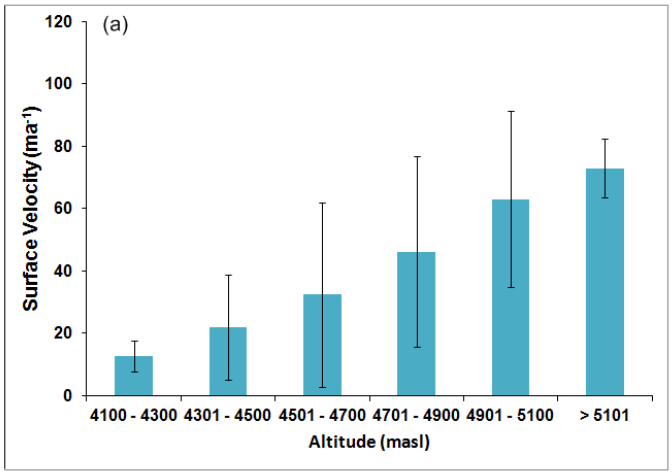

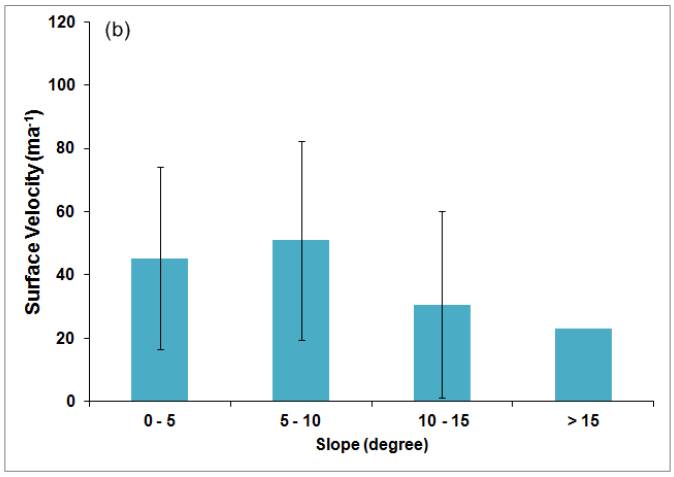

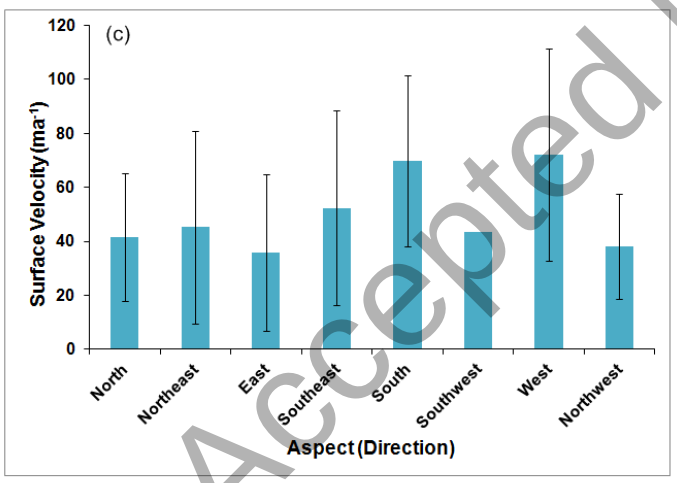

Figure 9. Relationship between the glacier surface velocity of the observed fixed points over the selected glaciers and spatial characteristics such as (a) altitude, (b) slope, and (c) aspect. (Detailed data is provided in supplementary table S2).

Table 1. Spatial characteristics, and annual velocity of studied glaciers of Chandra basin, western Himalaya.

Glacier ID	Glacier	Total area (km^2)	altitude (m asl)			Slope (°)			Annual surface velocity (ma^{-1})
			Min	Mean	Max	Min	Mean	Max	(mean ± SD)
A	Samudra Tapu	78.9	4200	5150	6100	3.5	12	30	64.3 ± 36.7
B	Sutri Dhaka	19.6	4400	5300	6200	2	14.3	35	52.6 ± 17.3
C	Batal	4.4	4240	5020	5800	6.2	10	16.2	6.2 ± 2.9
D	Gepang Gath	11.1	4000	4750	5500	5	15	35	26.5 ± 12.9